Retrofit Design of CO_2 Compression and Purification Process Using Intensification with Cryogenic Air Separation Unit

Koohestanian, Esmaeil
Department of Chemical Engineering, Iranshahr Branch, Islamic Azad University, Iranshahr, I.R. IRAN

Shahraki, Farhad*[+]
Department of Chemical Engineering, University of Sistan and Baluchestan, Zahedan, I.R. IRAN

ABSTRACT: *The CO_2 Compression and Purification Unit (CPU) is an auto refrigeration system that works based on the Joule-Thomson effect, which requires high energy for compression and refrigeration. Therefore, optimization of this system has been an attractive research field in recent years. However, this system is applied for capturing CO_2 from Oxy-Fuel Combustion (OFC) flue gases. The OFC refers to fuel combustion with approximate pure oxygen which in practice is usually produced from a cryogenic air separation unit (ASU). In this study, CO_2CPU system was redesigned based on oxygen stream effluent from cryogenic ASU. The results obtained by analyzing a sample of combustion gas showed that only the oxygen gas stream produced in the ASU unit, which is being prepared to enter the combustion chamber is sufficient to condense and refrigerate the CO_2CPU system. The performance of the proposed design was compared with three recently proposed schemes for a given feed. The results showed that the proposed system can perform at lower operating pressure and needs a significantly smaller heat-transfer area. In addition, the integration of CPU and ASU decreased the number of compressors and reduced the heat exchange area of cold boxes by at least 79% and the compressor energy consumption by at least 29%. It also allowed the delivery of the final CO_2 product in the subcooled liquid phase. Therefore, instead of the expensive compressor, the pump can be used to increase the pressure to transfer CO_2. Furthermore, optimization and sensitivity analysis were performed on this system using the Response Surface Methodology (RSM),which indicated that the inlet pressure and the temperature of the second separator had the most significant effect on this system.*

KEYWORDS: *CO_2 capture; CO_2CPU; Process design; Oxy-fuel combustion; Retrofit design; Global warming, Intensification.*

INTRODUCTION

Due to the continuous increase in the earth's average surface temperature and the major contribution of CO_2 to this greenhouse effect, separation of CO_2 from waste gas produced by combustion has taken on great importance,

* *To whom correspondence should be addressed.*
+ *E-mail: koohestanian@pgs.usb.ac.ir*
1021-9986/2023/2/552-563 12/$/6.02

both environmentally and economically. Electricity and heat production, by accounting 42% of the globally emitted CO_2, is the main cause of CO_2 emission. Also, more than 65 % CO_2 emission are resulted from combusting a considerable amount of fossil fuels, which show the significant effect of these processes on climate change [1].

Depending on gas stream conditions such as temperature, pressure, the concentration of CO_2 in flue gases, and the fuel type (solid or gas), the following three general methods are presented for Carbon Capture and Storage (CCS) from primary sources [2]: pre-combustion, post-combustion and oxy-fuel combustion (OFC). OFC carbon capture technology is considered as one of the most promising technique that both new and existing power plants can use to achieve a near-zero CO_2 emission [3]. This method, uses recycled flue gas and high purity O_2 (about 85%-98%), which usually obtained from ASU. Using O_2 instead of air in the furnace boosts combustion efficiency [4], which decreases fuel consumption and produces a high CO_2 concentration stream (more than 80% vol.) which enables easier purification through mechanical separation using the difference in the condensing temperatures instead of the absorption-based separation [5]. However, high purity O_2 also increases the flame temperature by about 3500°C which may damage the furnace [6]. Therefore, in the OFC, high-purity O_2 is diluted by the recycled flue gases (wet or dry) to control the flame temperature at the required level set by boiler metallurgical constraints [7].

Oxygen production, usually provided by cryogenic ASU, requires high refrigeration duty [8] and it is expected 3%-4% energy penalty for O_2 production using ASU [9]. There are other methods, such as advanced ceramic membrane (145.0 kWh/t O_2), to produce O_2 with lower energy and capital cost [10]. However, there are additional challenges in flux and O_2 purity in the case of ceramic and polymeric membranes, respectively [11]. Therefore, the ASU based on cryogenic distillation is still the most suitable approach to produce large volumes of high-purity O_2 [11].

The most widely used process in the OFC technology is the use of CO_2CPU suggested by International Energy Agency Greenhouse Gas (IEAGHG) R&D Programme [12]. The CO_2CPU is an auto refrigeration process that, with the help of the Joule-Thomson effect, reduces the pressure by passing the flow through a throttling valve, which in turn reduces the temperature. It requires high energy for compression, which increases the capital and operating costs [13]. Minimizing the operating costs can improve process economics, higher energy efficiency and reduced carbon emissions to the environment [14]. However, the CO_2CPU process is used to limit CO_2 in the OFC process. Therefore, in this research, the CO_2CPU system has been redesigned using the current streams in the OFC.

While there have been many numbers of researches conducted on CO_2CPU systems issues, a few studies have focused on the improvements of the CO_2CPU process flowsheet. Therefore, this research focused on the modification of the performance of OFC system through improvements of the CO_2CPU process. Through integrating system components such as the oxygen stream from the ASU and CO_2CPU, the process is optimized to capture CO_2 while minimizing the overall energy demand of these units and, subsequently, the plant's capital and operating costs.

THEORETICAL SECTION

Simulation details and method

CO_2CPU flowsheet description

OFC flue gases are mainly composed of steam water and CO_2, out of which the CO_2 can be captured without difficulty via cooling and condensation. However, a CO_2CPU process is still required to decrease the amount of unreacted O_2 and other non-condensable gases and meet the CO_2 quality requirements for transportation and storage [15]. This process is appropriate for capturing CO_2 from OFC flue gases which contain a high CO_2 portion. Although several Process Flow Diagrams (PFD) have been offered for the CPU system, the CO_2CPU process equipped with two flash drums is selected for OFC applications. In terms of the total cost of clean power production, this unit is similar to post-combustion CO_2 capture using an amine scrubbing process [16]. Fig. 1 shows the process flowsheet of CO_2CPU, an auto-refrigerated system designed based on the Joule-Thomson effect [17]. To avoid pipes and tubes' erosion resulting from hydrate formation and decrease the equipment's corrosion, the flue gas should be cooled and dehydrated before it is fed to this unit [18].

Due to the compressor volumetric efficiency decrease with a significant increase in compression ratio [19],

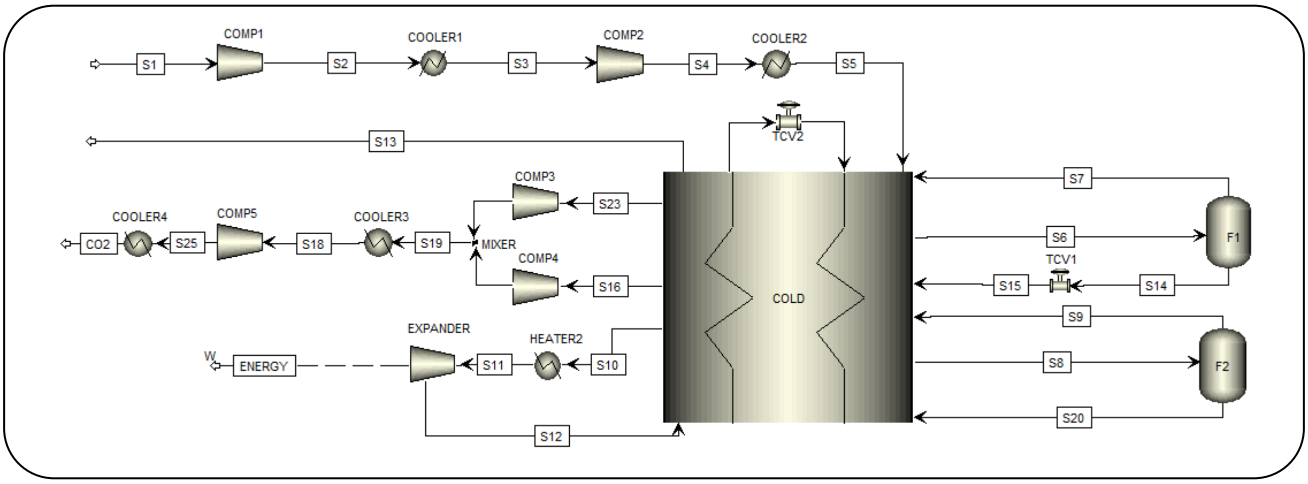

Fig. 1: PFD of CO_2CPU process.

compressing is done in two compressors equipped with intercoolers or a multi-stages compressor (MSC). The volumetric efficiency decreases with an increase in the compression ratio, leading to limiting discharge pressure. Optimum minimum horsepower is obtained when the compression ratio is the same in all cylinders for MSC [20]. Intercoolers are commonly used on the MSC to decrease the gas temperature to the original suction temperatures with a little pressure drop (about 5 psi) [21]. The number of compression stages can be calculated using Eq. (1) [22]:

$$\frac{P_2}{P_1} = k^n \tag{1}$$

Where *n* represents the number of stages, and *k* indicates the compression ratio.

Proposed process description

In this research, through integrating system components such as oxygen stream from the ASU and CO_2CPU, the process is optimized to capture CO_2 while minimizing the overall energy demand of these units and subsequently, the plant's capital and operating costs. Design limitations are as bellow [23]:

- The temperature in the process should be above the freezing point of CO_2 (-56.6°C).

- The minimum molar CO_2 purity in the product gas must be 95% [24]. Considering the operating temperatures of the separators, namely, -55°C and -35°C, respectively, in which CO_2 will occur in liquid phase, there is no concern regarding the violation of this condition.

- The recovery rate should not be less than 90%.

- The product gas should be delivered at 110 bar.

- The output flow pressure from the turbine should be approximately 1.5 bar, as it is assumed here that the stream from the turbine enters a capture unit for further recovery. Otherwise, the pressure can be reduced to atmospheric pressure, which will increase power generated and will improve energy integration.

Fig. 2 illustrates block diagram of relevant OFC and process proposed in this study. In this research, the CO_2CPU system has been retrofitted using the integration streams in OFC unit. In OFC process, high purity oxygen is usually supplied from the cryogenic ASU in the liquid phase, which boils at -195 ° C. However, to use oxygen in OFC, oxygen in the gas phase is required. Therefore, instead of using the throttle valve, the oxygen output of ASU is used as a coolant in the cold box.

Fig. 3 illustrates the PFD of CO_2CPU designed in this study. Data of the flue gas was extracted from the literature [25]. The dehydrated flue gas (S1) compressed through a two-stage compressor and entered to the cold-box at 203°C (stream S4). A pressure drop of 0.21 bar has been assumed through the cold-box [25]. Stream S4 is cooled down to -35°C, and then enters the first separator (F1) to separate the liquefied CO_2. The separators are assumed adiabatic and the pressure drop inside them has been neglected. Liquid oxygen stream effluent from cryogenic ASU as refrigerant inlet to the cold-box in -195 °C and 10 bar.

Although greater cooling is achievable, we cautiously chose this temperature to prevent CO_2 from freezing (which occurs at -56.6°C) and avoid hydrate formation and erosion of the pipes. The stream from top of the first separator (S6) is cooled to -55°C and fed to the second

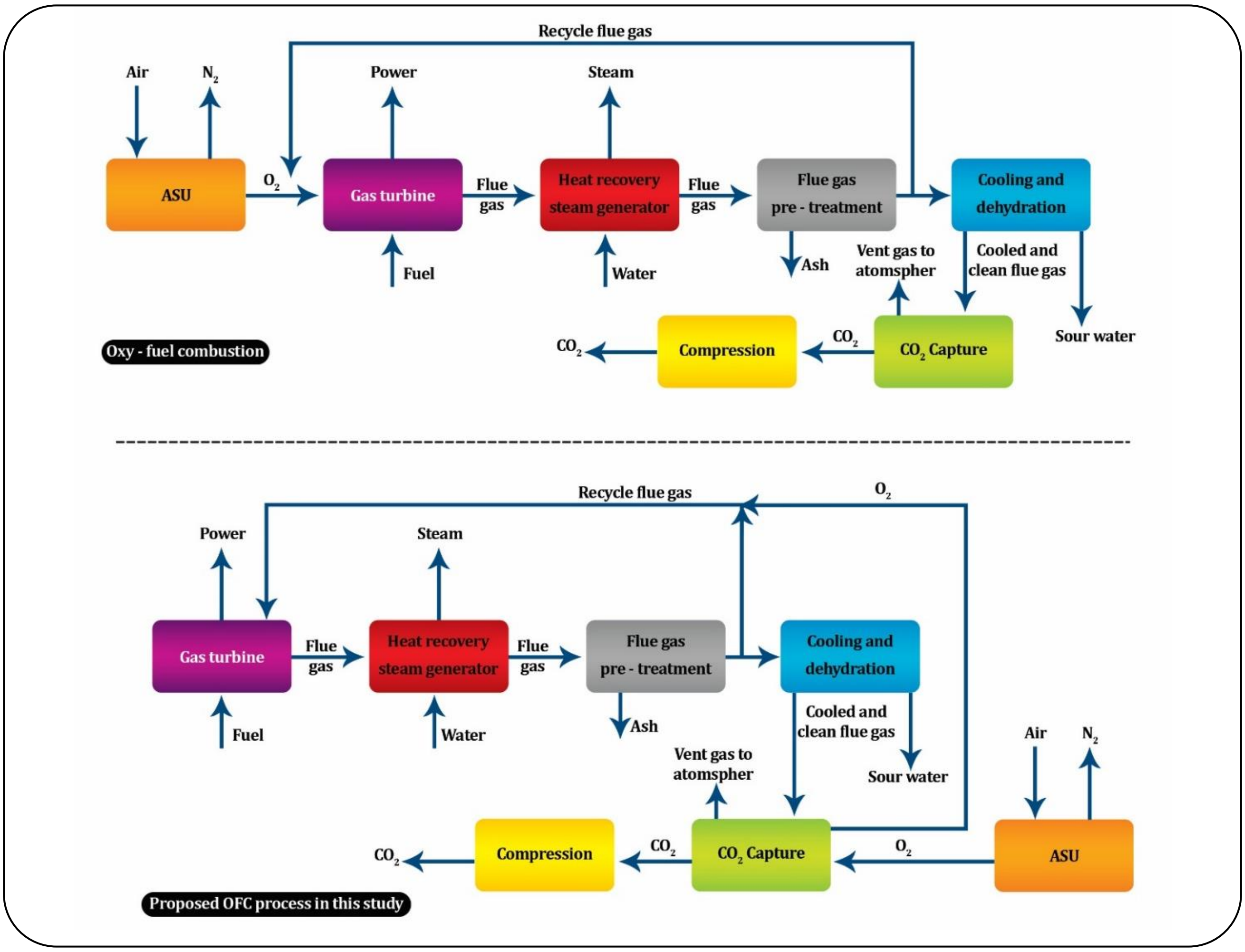

Fig. 2: Block diagram of relevant OFC and process proposed in this study.

separator (S8). The molar purity of CO_2 in the final product needs to be greater than 95% [26]. In the operating pressure of 25 bar, CO_2 occurs in liquid state, therefore eliminating the concerns about the purity of the final CO_2 product. The results for CO_2 purity in the final product confirm this.

The high-pressure stream from the top of the second separator (S9) enters the cold box. In exchange for this reduced pressure, power is generated in a turbine. Since turbines are expensive equipment, and to decrease fluctuations in the stream fed to the turbine, the stream is heated to 185°C in a cold-box. This increased temperature will also help to increase the power generated. The stream leaves the turbine (VENT) at 1.5 bar and 8.2°C. This stream can be fed to an amine- or ammonia-based CO_2 capture unit.

At last, all CO_2 products from the bottom of the two separators are mixed and pressurized to be permanently stored or utilized through pipelines in the form of gas phase, supercritical (dense) phase or subcooled liquid state. Both operating conditions and impurity content have a significant effect on CO_2 fluid properties. Furthermore, temperature changes have greater effect than pressure changes [27]. CO_2 density may significantly change with a small change in the operating conditions near CO_2 critical point. For instance, a reduction of about 10 °C from the critical temperature will have the double density [28]. Hence, CO_2 transported via pipeline is one of the highest amount in the dense phase. The critical temperature and pressure of CO_2 are 31.1°C and 7.38 MPa respectively. The minimum pressure of a CO_2 pipeline is about 10%, greater than the critical pressure of the flowing fluid [29].

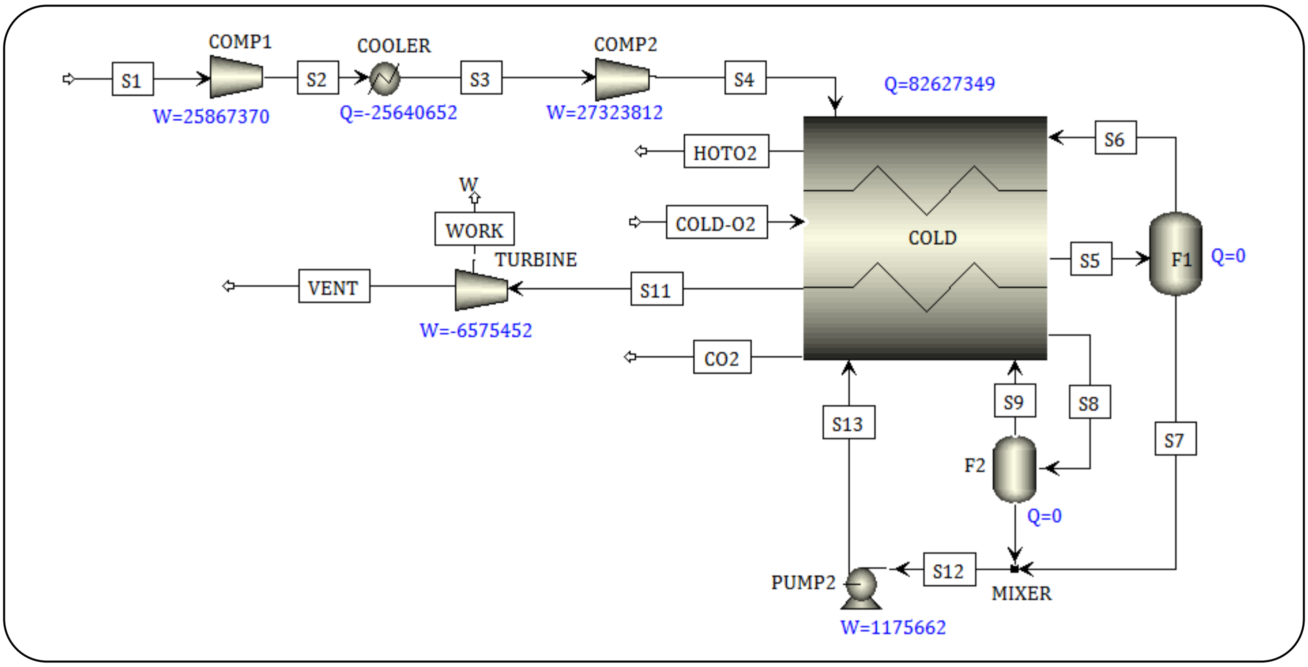

Fig. 3: PFD of the proposed structure.

However, even an ordinary change in the ambient temperature (or soil temperature in a buried pipeline) can lead to a two-phase mixture in the pipeline, which is required to be prevented [30]. However, if the pressure is more significant than 9.6 MPa, it can guarantee that CO_2 will be transported in the supercritical state at any temperature [31].

In this process design, the final product is available in the liquid phase at a temperature of -38 °C, which makes it possible to increase the pressure through using pump instead of the expensive compressors. The CO_2 streams from bottom of separators (namely, S7 and S10) merge together and pressurized to 11 MPa for permanently stored or utilized through pipelines in the form of subcooled liquid state.

Process modeling

After direct water cooling and dehydration, most of these impurities and dust are removed, and the significant components of the stream will include CO_2, N_2, and O_2. Therefore, the OFC flue gases can be regarded as a mildly nonpolar mixture. As a result, Peng-Robinson (PR) [32] and Soave-Redlich-Kwong (SRK) [33] thermodynamic equation of state (EOS) were recommended by AspenTech for these mildly nonpolar mixtures [34]. However, the PR was selected as the most appropriate EOS to estimate the thermo-physical specification of CO_2 stream containing a spot of impurities and the range of temperatures (−60°C - 250°C) and pressures (1bar-120 bar) [35]. The temperature-dependent binary parameters (k_{ij}) were modified accordingly, using the experimental data [1].

The present study uses the quadratic model of RSM associated with the D-Optimal design to optimize the operating condition of CPU process. Three parameters in three levels for each one, at different points of processes, are considered to propose an optimal operational condition. The parameters are flue gas pressure before the inlet to cold-box (A), the first separator temperature (B), and the second separator temperature (C). These parameters are optimized for the maximization of removal efficiency of CO_2 recovery (R1). Upper and lower levels of operating parameters are listed in Table 1 so that the range of these parameters was selected with respect to the process issues and previous studies. Since no liquefaction is possible at the pressures below the triple point, temperatures about below -56 °C must be avoided in order to prohibit the formation of solid carbon dioxide in the CO_2CPU. Considering the dew point temperature at the outlet of the compressor, the temperatures more than -27 °C should not be examined due to the lack of condensation and separation of CO_2, at the lowest pressure 20 bar.

Also, the recovery rate in each structure was calculated using Eq. 2:

$$\text{Recovery} = \frac{\text{Total CO}_2\text{in product stream}}{\text{Total CO}_2\text{in feed stream}} \tag{2}$$

These two stages will keep compressor discharge temperature below the maximum allowable temperature. The maximum allowable temperature can be set either by characteristics of the compressor cylinder or by the gas specifications such as temperature decomposition, or auto ignition [36]. According to CO_2 physical properties, the maximum allowable temperature can be considered as 260°C [37].

RESULTS AND DISCUSSION

Sensitivity analysis

Table 2 shows the results for each of the process conditions suggested by the RSM design.

Data obtained from simulations were investigated for R1 using the models named linear, two-factor interaction (2FI), quadratic and cubic. Furthermore, considering the values of standard deviation, higher R^2, adjusted R^2 and predicted R^2 of the quadratic model were found for response. The results of ANOVA analysis for selecting the model of R1 is shown in Table 3.

The criteria used in the selection of the appropriate model was the p-value of the model (P-vale <0.05), the p-value of the lack of fit (>0.05) and the coefficient of determination R^2(> 0.9). The p-value of the model (<0.05) means that the probability of being an incorrect model is less than 5%. According to Table 3, statistical analysis results show that A, B, and C, independently affect the process, as seen in Eq. 3. Therefore, according to the hierarchical principle, their effects and their interaction effects must be considered in the mathematical model.

$$\text{Recovery} = 0.4275 + 0.037617\text{P}_{\text{in}} + 0.000161\text{T}_{\text{F1}} - 0.02509\text{T}_{\text{F2}} - 5.2\times10^{-7}\text{P}_{\text{in}}\text{T}_{\text{F1}} + 0.000303\text{P}_{\text{in}}\text{T}_{\text{F2}} - 9.38\times10^{-7}\text{T}_{\text{F1}}\text{T}_{\text{F2}} - 0.000312\text{P}_{\text{in}}^2 + 7.0646\times10^{-5}\text{T}_{\text{F1}}^2 - 8.6\times10^{-5}\text{T}_{\text{F2}}^2 \tag{3}$$

The 3D diagram for further investigation of these effects is illustrated in Fig. 4. The results show that the inlet pressure (A) and second separator temperature (C) have the most important effect on recovery (R1).

According to the Fig. 4, parameters A and C have the greatest effect on the R1. According to Fig. 4a, increasing

Table 1: Simulation range.

	Simulation range	
Process factor	Lower level	Upper level
A (bar)	25	35
B (°C)	-45	-30
C (°C)	-55	-45

Table 2: RSM results for each of the process conditions.

Run	A	B	C	R1
1	27.5	-37.5	-43.75	0.885578
2	25.0	-45.0	-55.00	0.930907
3	35.0	-30.0	-40.00	0.899590
4	25.0	-45.0	-47.50	0.895600
5	30.0	-37.5	-47.50	0.917578
6	25.0	-30.0	-40.00	0.830249
7	35.0	-30.0	-55.00	0.952498
8	35.0	-45.0	-55.00	0.954815
9	30.0	-37.5	-55.00	0.943996
10	25.0	-30.0	-55.00	0.928571
11	30.0	-37.5	-47.50	0.917578
12	35.0	-37.5	-47.50	0.933149
13	30.0	-30.0	-47.50	0.915675

Table 3: ANOVA analysis for selecting the model of R1.

Source	Sum of Squares	F-value	p-value
Model	0.013259	696.6985	< 0.0001
A	0.002201	1040.754	< 0.0001
B	3.91×10^{-5}	18.50266	0.0231
C	0.00092	435.0433	0.0002
AB	1.58×10^{-7}	0.074652	0.8024
AC	0.00052	246.0118	0.0006
BC	2.34×10^{-5}	11.07376	0.0448
A^2	5.08×10^{-5}	24.00231	0.0163
B^2	1.39×10^{-5}	6.576135	0.0829
C^2	1.48×10^{-5}	6.992101	0.0774

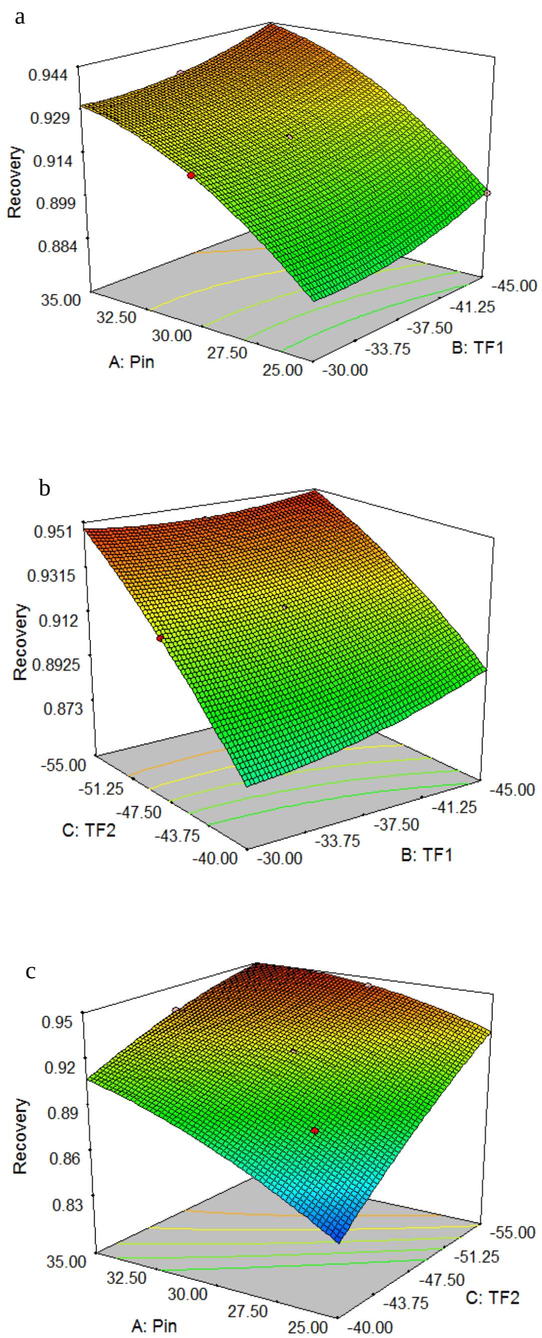

Fig. 4: System performance under variations of parameters vs CO_2 recovery, R1.

the pressure to 35 bar caused an increasing the CO_2 production rate with a relatively sharp slope, which eventually decreased at the end of the diagram due to the CO_2 content deduction in the process. According to this figure, the effective range of pressure change can be limited to the range of 25 to 35 bar. While parameter B has no significant effect on CO_2 recovery rate.

As shown in Fig. 4b, as the temperature of the second separator decreases from -40°C to -55°C, the value of R1 increases due to the increase in the condensate rate. However, the temperature of the first separator does not affect the amount of recovered CO_2.

Finally, as clearly shown in Fig. 4c, parameters A and C have the greatest impact on the R1. According to this figure, increasing the inlet pressure and decreasing the temperature of the second separator will lead to a significant increase in R1. However, pressures above 35 bar cause other components to liquefy, so there will be virtually no separation. Also, if purified CO_2 is used in processes such as enhace oil recovery, urea synthesis or methanol production, due to some technical, process and economic considerations such as efficiency changes, safety issues, environmental issues and corrosion reduction, minimum CO_2 purity should be 95% [38], which was applied as one of the constraints in the objective function.

Finally, the optimal MSC discharge pressure was found as 25 bar the optimal first and second flash drum temperatures were also obtained -45 °C, and -55 °C, respectively.

Process analysis

The results of steady-state process output based on the feed composition in the study of *Jin et al.* [25] have been summarized in Appendix A. The composite curves for the streams within the cold-box (Fig. 5) confirms that no temperature cross has occurred and the curves are in appropriate distances from each other, ensuring the absence of a temperature cross. The CO_2 purity and recovery in the product were about 97%, and 90%, respectively, which were desirable.

The results of the comparison of the four schemes have been presented in Table 4. The PFD proposed in the present study provides a greater purity as well as having a decreased maximum operating pressure (MOP) and heat transfer area (A). Decreased MOP and A will contribute to reduced operational and investment costs [1]. Although the recovery rate in our structure was slightly lower than others, the difference is negligible.

Table 4: Comparison of the CO_2CPU design.

		Luyben study [39]	Jin et al. study [25]	Koohestanian et al. study [23]	This research
Cold-Box 1	Duty (MW)	5.108	27.525	56.858	85.985
	LMTD (K)	11.04	4.94	17.00	133
	A (m^2)	2721	32786	19674	3880
Cold-Box 2	Duty (MW)	25.910	22.007	-	-
	LMTD (K)	4.71	4.1	-	-
	A(m^2)	32320	31750	-	-
Cold-Box 3	Duty (MW)	21.400	-	-	-
	LMTD (K)	5.71	-	-	-
	A(m^2)	22000	-	-	-
Purity %		95.17	96.65	96.74	96.90
Recovery %		90.29	90.82	90.08	89.34
MOP (bar)		30	30	29	25
No. of gas compressor		6	4	6	2
Compressor work (MW)(1)		63.489	81.289(2)	94.235	45.191
Total cold-box area (m^2)		57041	64536	19674	3880

(1) For all design final pressure suppose 110 bar, and vent gas warm to 301 °C before inlet to expander.
(2) In Jin design compressor work may decrease to 72.441MW if expander replace to CO_2 vent gas.

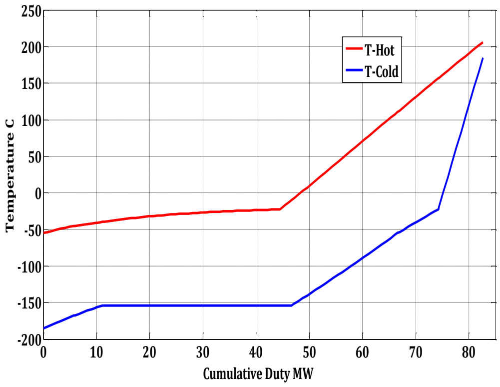

Fig. 5: The composite curve for the cold-box in the new scheme.

Rubber or carbon steel become brittle in contact to this material. The sudden evaporation of this liquid also creates a huge force. If the cooling cycle outlets are clogged or if the refrigerator compartment or storage compartment is completely seamless, the pressure will rise too much and an explosion will occur.

CONCLUSIONS

In the present study, a new structure was proposed and developed for CO_2CPU unit. As the new scheme utilizes less equipment compared to other suggested structures, it decreases investment costs by reducing the number of cold boxes and improving energy integration.

Here, the performance of the proposed design was compared with that of three recently presented schemes for a given feed. The results showed that, compared with the other designs, the proposed system in this research not only can perform at lower operating pressure but also needs a significantly smaller heat transfer area. Furthermore, the availability of the final product using the proposed process flow diagram in the liquid phase at a temperature of -38 °C makes it possible to increase the pressure by using a pump instead of expensive compressors. In addition, pressurizing liquefied CO_2 requires less energy compared to gaseous CO_2 because a specific volume of liquid CO_2 is reduced compared to gaseous CO_2. The integration of CPU and ASU also decreases the number of compressors and reduces the heat exchange rate of cold-boxes and compressor energy consumption by at least 79% and 29%, respectively.

Appendix A

Table A1: Mass and energy balance for the new process based on feed composition used in Jin et al. [27].

Stream no.	S1	S2	S3	S4	S5	S6
Temperature °C	20.0	186.7	25.0	203.1	-45.0	-45.0
Pressure bar	1.1	5.28	4.935	25.44	25.23	25.23
Vapor Frac.	1	1	1	1	0.248	1
Mass flow kg/hr	717.187	717.187	717.187	717.187	717.187	154.556
Composition Mole Frac.						
CO_2	0.824	0.824	0.824	0.824	0.824	0.386
O_2	0.042	0.042	0.042	0.042	0.042	0.142
N_2	0.095	0.095	0.095	0.095	0.095	0.337
Ar	0.039	0.039	0.039	0.039	0.039	0.134
CO (ppm)	31	31	31	31	31	110
SO_2	14 ppm	14 ppm	14 ppm	14 ppm	14 ppm	675 ppm
SO_3 (ppb)	83	83	83	83	83	trace
NO (ppm)	20	20	20	20	20	61
NO_2	20 ppm	20 ppm	20 ppm	20 ppm	20 ppm	117 ppb

Stream no.	S7	S8	S9	S10	S11	S12
Temperature °C	-45.0	-55.0	-55.0	-55.0	185.0	-45.5
Pressure bar	25.23	25.02	25.02	25.02	24.81	25.02
Vapor Frac.	0	0.833	1	0	1	0.001
Mass Flow kg/hr	562.631	154.556	123.573	30.983	123.573	593.614
Composition Mole Frac.						
CO_2	0.969	0.386	0.27	0.964	0.27	0.968
O_2	0.009	0.142	0.169	0.01	0.169	0.009
N_2	0.015	0.337	0.402	0.017	0.402	0.015
Ar	0.008	0.134	0.16	0.009	0.16	0.008
CO (ppm)	5	110	131	6	131	5
SO_2	18 ppm	675 ppb	77 ppb	4 ppm	77 ppb	18 ppm
SO_3 (ppb)	110	trace	trace	1	trace	105
NO (ppm)	7	61	71	9	71	7
NO_2	27 ppm	117 ppb	1 ppb	695 ppb	1 ppb	25 ppm

Stream no.	S13	CO2	COLD-O2	HOT-O2	VENT
Temperature °C	-31.9	-55.0	-185.0	4.9	8.2
Pressure bar	110.0	109.8	10.0	9.8	1.5
Vapor Frac.	0	0	0	1	1
Mass Flow kg/hr	593.614	593.61	922.00	922.00	123.573
Composition Mole Frac.					
CO_2	0.968	0.968			0.27
O_2	0.009	0.009	1	1	0.169
N_2	0.015	0.015			0.402
Ar	0.008	0.008			0.16
CO (ppm)	5	5			131
SO_2	18 ppm	18 ppm			77 ppb
SO_3 (ppb)	105	105			trace
NO (ppm)	7	7			71
NO_2	25 ppm	25 ppm			1 ppb

Received : Feb. 18, 2022 ; Accepted : Apr. 25, 2022

REFERENCES

[1] Koohestanian E., Shahraki F., Review on principles, recent progress, and future challenges for oxy-fuel combustion CO_2 capture using compression and purification unit, *Journal of Environmental Chemical Engineering*, 105777 (2021).

[2] Gaurina-Međimurec N., Novak-Mavar K., Majić M., Carbon Capture and Storage (CCS): Technology, Projects and Monitoring Review, *Rudarsko-Geolosko-Naftni Zbornik*, **33(2)**: 1-15 (2018).

[3] González-Salazar M.A., Recent Developments in Carbon Dioxide Capture Technologies for Gas Turbine Power Generation, *International Journal of Greenhouse Gas Control*, **34**: 106-116 (2015).

[4] Hong J., et al., Analysis of Oxy-Fuel Combustion Power Cycle Utilizing a Pressurized Coal Combustor, *Energy*, **34(9)**: 1332-1340 (2009).

[5] Darde A., et al., Air Separation and Flue Gas Compression and Purification Units for Oxy-Coal Combustion Systems, *Energy Procedia*, **1(1)**: 527-534 (2009).

[6] Chansomwong A., Dynamic Modelling of a CO_2 Capture and Purification Unit for Oxy-Coal-Fired Power Plants, University of Waterloo (2014).

[7] Wu F., et al., Progress in O_2 Separation for Oxy-Fuel Combustion-A Promising Way for Cost-Effective CO_2 Capture: A Review, *Progress in Energy and Combustion Science*, **67**: 188-205 (2018).

[8] Mehrpooya M., Sharifzadeh M.M.M., Mousavi S.A., Evaluation of an Optimal Integrated Design Multi-Fuel Multi-Product Electrical Power Plant By Energy and Exergy Analyses, *Energy*, **169**: 61-78 (2019).

[9] Shah K., et al., Integration Options for Novel Chemical Looping Air Separation (ICLAS) Process for Oxygen Production in Oxy-Fuel Coal Fired Power Plants, *Fuel*, **107**: 356-370 (2013).

[10] Pfaff I., Kather A., Comparative Thermodynamic Analysis and Integration Issues of CCS Steam Power Plants Based on Oxy-Combustion with Cryogenic or Membrane Based Air Separation, *Energy Procedia*, **1(1)**: 495-502 (2009).

[11] Nemitallah M.A., et al., Oxy-Fuel Combustion Technology: Current Status, Applications, and Trends, *International Journal of Energy Research*,. **41(12)**: 1670-1708 (2017).

[12] Dillon D., et al., Oxy-Combustion Processes for CO_2 Capture from Power Plant, *Engineering Investigation Report*, **9**: (2005)

[13] Mokhatab S., et al., Handbook of Liquefied Natural Gas, Gulf Professional Publishing (2013).

[14] Montanez-Morantes M., Jobson M., Zhang N., Operational Optimisation of Centrifugal Compressors in Multilevel Refrigeration Cycles, *Computers & Chemical Engineering*, **85**: 188-201 (2016).

[15] Wetenhall B., Race J., Downie M., The effect of CO_2 Purity on the Development of Pipeline Networks for Carbon Capture and Storage Schemes, *International Journal of Greenhouse Gas Control*, **30**: 197-211 (2014).

[16] Ciferno J., Pulverized Coal Oxycombustion Power Plants. Final Report, August, (2007).

[17] Sonntag R.E., et al., Fundamentals of Thermodynamics. Vol. 6., Wiley New York (1998).

[18] Choi Y.-S., Nešić S., Effect of Water Content on the Corrosion Behavior of Carbon Steel in Supercritical CO_2 Phase with Impurities, *Corrosion* 2011, (2011).

[19] Noh K.-Y., et al., Compressor Efficiency with Cylinder Slenderness Ratio of Rotary Compressor at Various Compression Ratios, *International Journal of Refrigeration*, **70**: 42-56 (2016).

[20] Hashemi E., Pezeshkpour P., "Multi-Stage Centrifugal Compressors and Defining the Optimum Pressure Ratio According to Temperature Limitations", in *ASME Power Conference*. (2008).

[21] Seider W.D., Seader J.D., Lewin D.R., Product & Process Design Principles: Synthesis, Analysis and Evaluation, (with CD), John Wiley & Sons (2009).

[22] Ludwig E.E., "Applied Process Design for Chemical and Petrochemical Plants", Vol. 2., Gulf Professional Publishing (1997).

[23] Koohestanian E., et al., New Process Flowsheet for CO_2 Compression and Purification Unit; Dynamic Investigation and Control, *Iranian Journal of Chemistry and Chemical Engineering (IJCCE)*, **40(2)**: 593-604 (2021).

[24] De Visser E., et al., Dynamis CO_2 Quality Recommendations, *International Journal of Greenhouse Gas Control*, **2(4)**: 478-484 (2008).

[25] Jin B., Zhao H., Zheng C., Optimization and Control for CO_2 Compression and Purification Unit in Oxy-Combustion Power Plants, *Energy*, **83**: 416-430 (2015).

[26] De Visser E., et al., Dynamis CO_2 Quality Recommendations. Dynamis Project, 6^{th} Framework Programme, The Netherlands, p. 16-35 (2007).

[27] Liu S., et al., Density Characteristics of CO_2–CH_4 Binary Mixtures at Temperatures from (300 to 308.15) K and Pressures from (2 to 18) MPa, *The Journal of Chemical Thermodynamics*, **106**: 1-9 (2017).

[28] Onyebuchi V.E., et al., A Systematic Review of Key Challenges of CO_2 Transport via Pipelines, *Renewable and Sustainable Energy Reviews*, **81**: 2563-2583 (2018).

[29] Lemontzoglou A., et al., Analysis of CO_2 Transport Including Impurities for the Optimization of Point-To-Point Pipeline Networks for Integration into Future Solar Fuel Plants, *International Journal of Greenhouse Gas Control*, **66**: 10-24 (2017).

[30] Kurz R., Ohanian S., Brun K., "Compressors in High-Pressure Pipeline Applications. in ASME Turbo Expo 2010: Power for Land, Sea, and Air", American Society of Mechanical Engineers Digital Collection (2010).

[31] Lu H., et al., Carbon Dioxide Transport via Pipelines: a Systematic Review, *Journal of Cleaner Production*, 121994 (2020).

[32] Peng D.-Y., Robinson D.B., A New Two-Constant Equation of State, *Industrial & Engineering Chemistry Fundamentals*, **15(1)**: 59-64 (1976).

[33] Soave G., Equilibrium Constants from a Modified Redlich-Kwong Equation of State, *Chemical Engineering Science*, **27(6)**: 1197-1203 (1972).

[34] Aspen Plus, "Aspen Plus Documentation Version V7. 3". Aspen Tech, Cambridge, MA, USA, 2011.

[35]. Kolster C., et al., The role of CO_2 Purification and Transport Networks in Carbon Capture and Storage Cost Reduction, *International Journal of Greenhouse Gas Control*, **58**: 127-141 (2017).

[36] Ludwig E.E., "Applied Process Design For Chemical and Petrochemical Plants". Vol. 3., Gulf Professional Publishing (1997).

[37] Carl R.B., "Rules of Thumb for Chemical Engineers", USA: Gulf Publishing Company (1998).

[38] Koohestanian E., et al., A Novel Process for CO_2 Capture from the Flue Gases to Produce Urea and Ammonia, *Energy*, **144**: 279-285 (2018).

[39] Luyben, W.L., Simple Control Structure for a Compression Purification Process in an Oxy-Combustion Power Plant, *AIChE Journal*, **61(5)**: 1581-1588 (2015).